

Microstructural modifications induced by rapid thermal annealing in plasma deposited SiO_xN_yH_z films

A. del Prado, E. San Andrés, I. Mártil, G. González-Daz, D. Bravo, F. J. López, M. Fernández, and F. L. Martinez

Citation: [Journal of Applied Physics](#) **94**, 1019 (2003); doi: 10.1063/1.1586979

View online: <http://dx.doi.org/10.1063/1.1586979>

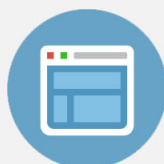
View Table of Contents: <http://scitation.aip.org/content/aip/journal/jap/94/2?ver=pdfcov>

Published by the [AIP Publishing](#)



Re-register for Table of Content Alerts

Create a profile.



Sign up today!



Microstructural modifications induced by rapid thermal annealing in plasma deposited $\text{SiO}_x\text{N}_y\text{H}_z$ films

A. del Prado,^{a)} E. San Andrés, I. Mártel, and G. González-Díaz
Departamento Física Aplicada III, Universidad Complutense de Madrid, 28040 Madrid, Spain

D. Bravo and F. J. López
Departamento Física de Materiales, Universidad Autónoma de Madrid, 28049 Madrid, Spain

M. Fernández
Instituto de Ciencia de Materiales, 28049 Cantoblanco, Spain

F. L. Martínez
Departamento Electrónica, Tecnología de Computadores y Proyectos, Universidad Politécnica de Cartagena, Cartagena 30202, Spain

(Received 23 April 2003; accepted 28 April 2003)

The effect of rapid thermal annealing (RTA) processes on the structural properties of $\text{SiO}_x\text{N}_y\text{H}_z$ films was investigated. The samples were deposited by the electron cyclotron resonance plasma method, using SiH_4 , O_2 and N_2 as precursor gases. For $\text{SiO}_x\text{N}_y\text{H}_z$ films with composition close to that of SiO_2 , which have a very low H content, RTA induces thermal relaxation of the lattice and improvement of the structural order. For films of intermediate composition and of compositions close to SiN_yH_z , the main effect of RTA is the release of H at high temperatures ($T > 700^\circ\text{C}$). This H release is more significant in films containing both Si–H and N–H bonds, due to cooperative reactions between both kinds of bonds. In these films the degradation of structural order associated to H release prevails over thermal relaxation, while in those films with only N–H bonds, thermal relaxation predominates. For annealing temperatures in the 500–700 °C range, the passivation of dangling bonds by the nonbonded H in the films and the transition from the paramagnetic state to the diamagnetic state of the *K* center result in a decrease of the density of paramagnetic defects. The H release observed at high annealing temperatures is accompanied by an increase of density of paramagnetic defects. © 2003 American Institute of Physics. [DOI: 10.1063/1.1586979]

I. INTRODUCTION

The requirements for ultralarge scale integration technology have stimulated the development of low thermal processes for the growth of dielectric films.^{1,2} One of the most extended techniques for the deposition of silicon oxynitride films (in the following $\text{SiO}_x\text{N}_y\text{H}_z$) at low temperatures is plasma enhanced chemical vapor deposition (PECVD),^{3–5} with the remote PECVD^{1,6,7} or electron cyclotron resonance (ECR-PECVD)^{8–11} variants.

While these techniques meet the low thermal budget requirement, the quality of the as-deposited dielectric films is not as good as that of thermally grown SiO_2 films.^{12,13}

Rapid thermal annealing (RTA) processes allow high temperature processing for a very short time, so the thermal budget is low, and they have been reported to improve the properties of dielectric films deposited at low temperatures.^{1,12–17}

Additionally, it is usual that H present in precursor gases (such as SiH_4 and NH_3) is incorporated into the deposited films during the PECVD process. The role of this H and of the thermal stability of the films during RTA is of great interest, because network reactions and relaxation processes

may be induced, thereby improving or degrading the properties of the films.

In previous work, our group has thoroughly studied the influence of RTA processes on the properties of SiN_yH_z films deposited by ECR PECVD.^{18–22} Different bonding rearrangement reactions that involve H bonds (Si–H and N–H bonds), depending on the film composition and structure of the bonds, are activated by the RTA process. If both Si–H and N–H bonds are present in the films, cooperative reactions between both kinds of bonds take place, so the mechanisms for the release of H are different from those in films with N–H bonds only. Additionally, the density of paramagnetic defects (basically the *K* center) is lowered and the electrical properties are improved for annealing temperatures in the 500–600 °C range. For higher annealing temperatures the release of H results in degradation of the properties of the films.

We have also previously studied the effects of RTA on SiO_2 and SiO_xH_z films.^{23,24} For stoichiometric H-free SiO_2 films, RTA results in thermal relaxation of the lattice and improvement of the structural order. On the other hand, for suboxide films ($x = [\text{O}]/[\text{Si}] \approx 1$), with a significant Si–H bond concentration, the release of H at annealing temperatures above 400 °C results in a significant increase of the concentration of Si dangling bonds.²⁴

^{a)}Electronic mail: alvarop@fis.ucm.es

Although silicon nitride and silicon oxide are extensively used in the microelectronics industry, silicon oxynitride emerges as a very interesting material due to the possibility to combine the properties of both materials.

In this work the influence of RTA on the structural properties and concentration of paramagnetic defects of $\text{SiO}_x\text{N}_y\text{H}_z$ films deposited by ECR PECVD is studied in detail. Samples with compositions over the whole range of $\text{SiO}_2\text{--SiN}_y\text{H}_z$ are analyzed. Special attention is devoted to the role of H: we studied samples with both Si–H and N–H bonds and samples with N–H bonds only.

II. EXPERIMENT

$\text{SiO}_x\text{N}_y\text{H}_z$ films were deposited using a commercial ECR reactor (Astex AX4500) attached to a stainless steel deposition chamber.²⁵ SiH_4 , O_2 and N_2 were used as precursor gases. The total gas flow, pressure and microwave power were kept constant at 10.5 sccm, 9×10^{-4} mbar and 100 W, respectively. The substrates were not intentionally heated and the deposition temperature was about 50 °C.

The films were deposited on high resistivity (80 Ω cm) *p*-type Si (111) substrates. The substrates were cleaned using standard procedures.²⁶ The thickness of the samples was about 100 nm for Auger electron spectroscopy (AES) and ellipsometry measurements. For the electron paramagnetic resonance (EPR) analysis stacks of films deposited by the same process to a total thickness of between 1500 and 2500 nm were used. Finally, Fourier transform infrared (FTIR) spectroscopy was performed on samples of 100, 300 and 500 nm.

Samples of different compositions were deposited by adjusting the gas flow ratios. In previous work we have shown that the main deposition parameters that control the $\text{SiO}_x\text{N}_y\text{H}_z$ composition in our process are the gas flow ratios: $R = [\phi(\text{O}_2) + \phi(\text{N}_2)] / \phi(\text{SiH}_4)$ and $Q = \phi(\text{O}_2) / \phi(\text{SiH}_4)$.^{11,27,28} The parameter R determines the Si content of the films, with higher Si contents for lower values of R . The parameter Q determines the relative incorporation of O and N, so the composition approaches that of SiO_2 as parameter Q is increased. Three different values of parameter R were used in this work: $R = 1.6$, 5.0, and 9.1. For each value of R , different samples with the parameter Q changed from $Q = 0$ to 4.5 were deposited. Those samples deposited at $R = 1.6$ have both Si–H and N–H bonds, while those deposited at $R = 5.0$ and 9.1 have N–H bonds only. Details of the influence of deposition parameters R and Q are given elsewhere.^{11,27,28}

In this work, the samples will be referred to as the values of parameters R and Q used during deposition (for instance, sample R1.6Q0.80 means that it was deposited at $R = 1.6$ and $Q = 0.80$).

After deposition, the wafers were cut in several 1×1 cm² samples in order to perform RTA treatment at different temperatures. Nonannealed samples were kept as references.

The RTA annealing processes were performed in a Modular Process Technology furnace, model RTP-600, equipped with a graphite susceptor. The samples were an-

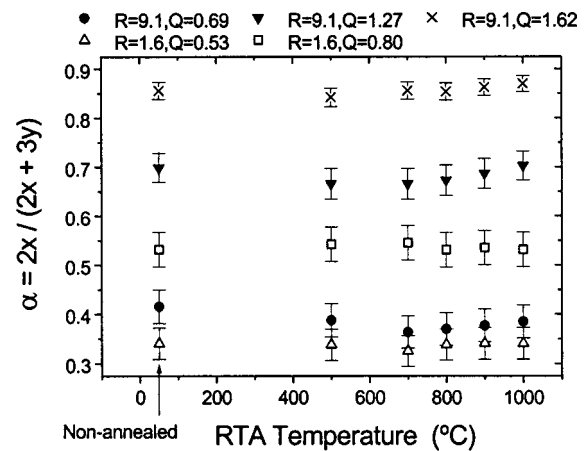


FIG. 1. Composition parameter $\alpha = 2x/(2x + 3y)$ determined by AES, as a function of the RTA temperature, for samples deposited at different gas flow ratios: $R = [\phi(\text{O}_2) + \phi(\text{N}_2)] / \phi(\text{SiH}_4)$ and $Q = \phi(\text{O}_2) / \phi(\text{SiH}_4)$.

nealed at temperatures ranging from 400 to 1000 °C for 30 s in argon atmosphere.

The composition of the samples was measured by AES using a JEOL system (JAMP-10S), with a 5 keV electron beam with a diameter of 0.1 mm at normal incidence. The samples were bombarded with 2 keV Ar^+ ions in order to reach the bulk of the film.

The structure of the bonds of the samples was analyzed by FTIR spectroscopy using a Nicolet Magna-IR 750 series II spectrometer working in transmission mode at normal incidence.

The thickness of the films and the refractive index at He–Ne laser wavelength of 632.8 nm were measured by ellipsometry using a Gaertner L116B ellipsometer with its incidence and detection angles both set at 70°.

Finally, the density of paramagnetic defects was analyzed by EPR measurements using a Bruker ESP 300E X band spectrometer. The microwave power was set at 0.5 mW to avoid saturation of the signal and the density of defects was evaluated using a weak pitch standard.

III. RESULTS

A. AES

We have shown in previous work that the composition of SiN_yH_z films is affected by RTA.^{18,21} For near stoichiometric ($y = [\text{N}]/[\text{Si}] = 1.43$) and Si-rich films ($y = [\text{N}]/[\text{Si}] = 0.97$), which show both Si–H and N–H bonds, the N/Si ratio decreases for annealing temperatures above 600 °C, as N is released in the form of NH_3 . On the other hand, the composition of N-rich films, with N–H bonds only, is unaffected by RTA up to 1050 °C.

In this work we have extended the composition measurements to $\text{SiO}_x\text{N}_y\text{H}_z$ films of intermediate and near SiO_2 compositions. The parameter $\alpha = 2x/(2x + 3y)$ was used to characterize the composition of the films. This parameter provides information about the relative amount of O and N or, in other words, about how close to silicon nitride or silicon oxide the composition is, with $\alpha = 0$ for Si_3N_4 and $\alpha = 1$ for SiO_2 .²⁸ Figure 1 shows the value of α for samples de-

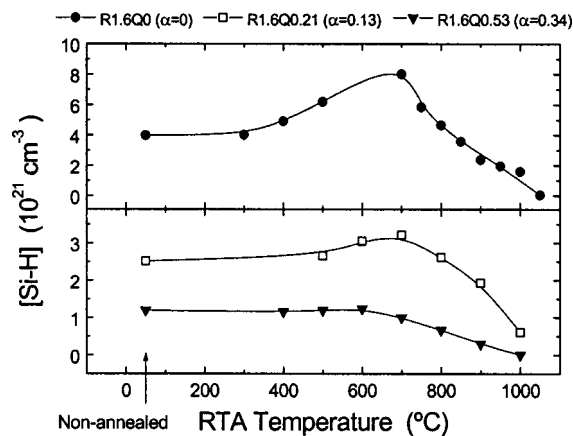


FIG. 2. Si–H bond concentration as a function of the RTA temperature for samples deposited at $R=1.6$ and different values of Q . The lines are a guide to the eye.

posited at different gas flow ratios as a function of the RTA temperature. No significant changes in α are observed for $\text{SiO}_x\text{N}_y\text{H}_z$ films in this range of compositions. So, it is concluded that the relative content of N and O is essentially unaffected for α values in the 0.3–1 range.

We have not observed any significant effect of RTA on the Si content of the films either.

B. FTIR spectroscopy

FTIR spectroscopy provides very useful information about the structure of bonds in the films. Absorption bands are observed for characteristic vibration frequencies of different molecular groups present in the films. The Si–H, N–H and O–H stretching bands allow the detection of H bonded in the films.

In our $\text{SiO}_x\text{N}_y\text{H}_z$ films, no O–H bonds were detected in any sample. Those samples deposited at $R=1.6$ show both Si–H and N–H bonds, with a higher N–H bond concentration, while those deposited at $R=5.0$ and 9.1 show N–H bonds only. The H concentration was estimated from these absorption bands using the calibration factors provided by Lanford and Rand.²⁹

Figure 2 shows the Si–H bond concentration as a function of the annealing temperature (T) for samples deposited at $R=1.6$, with different compositions, including SiN_yH_z . For the SiN_yH_z sample (R1.6Q0, $\alpha=0$), an increase of the Si–H bond concentration is observed for annealing temperatures up to 700°C . For higher temperatures the concentration decreases, and for $T>800^\circ\text{C}$ it becomes lower than in the nonannealed sample, being almost negligible for the highest temperature. The behavior of $\text{SiO}_x\text{N}_y\text{H}_z$ with composition closest to SiN_yH_z (sample R1.6Q0.23, $\alpha=0.13$) is very similar, although for this sample the Si–H bond concentration in the as-deposited sample (nonannealed) is lower and the increase of Si–H concentration for T up to 700°C is less significant. For sample R1.6Q0.53 ($\alpha=0.34$) the Si–H concentration is even lower and no significant increase of Si–H concentration is observed. As α is further increased, the Si–H bond concentration becomes lower, even below the

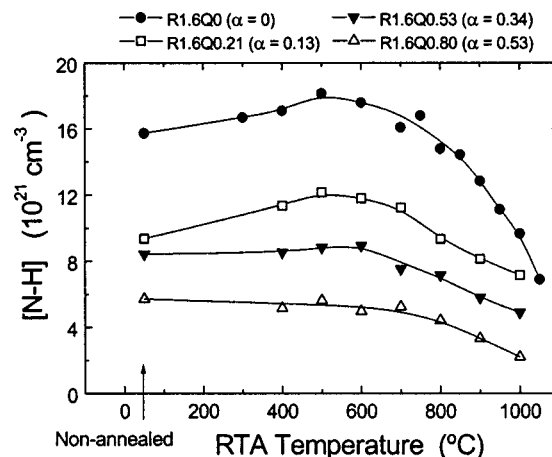


FIG. 3. N–H bond concentration as a function of the RTA temperature for samples deposited at $R=1.6$ and different values of Q . The lines are a guide to the eye.

detection limit for sample R1.6Q0.80, with $\alpha=0.53$, which is not shown.

The N–H bond concentration as a function of the RTA temperature for the samples deposited at $R=1.6$ is shown in Fig. 3. Sample R1.6Q0.80 ($\alpha=0.53$) is also included. For the SiN_yH_z sample (R1.6Q0, $\alpha=0$) there is a slight increase of N–H concentration for temperatures up to 500°C . For higher annealing temperatures the concentration decreases with respect to the maximum value and becomes lower than in the as-deposited film for $T>700^\circ\text{C}$. As in the case of the Si–H bond concentration, the behavior of sample R1.6Q0.21 ($\alpha=0.13$) is very similar to that of SiN_yH_z , with the maximum concentration of N–H bonds also observed for $T=500^\circ\text{C}$. For the samples of intermediate composition (samples R1.6Q0.53 with $\alpha=0.34$ and R1.6Q0.80 with $\alpha=0.53$) there is no significant increase of N–H concentration for low annealing temperatures.

Figure 4 shows the concentration of N–H bonds as a function of the annealing temperature for samples deposited at $R=5.0$ and 9.1 , in which no Si–H bonds were detected. Samples deposited at different values of Q (and therefore with different values of composition parameter α) are shown.

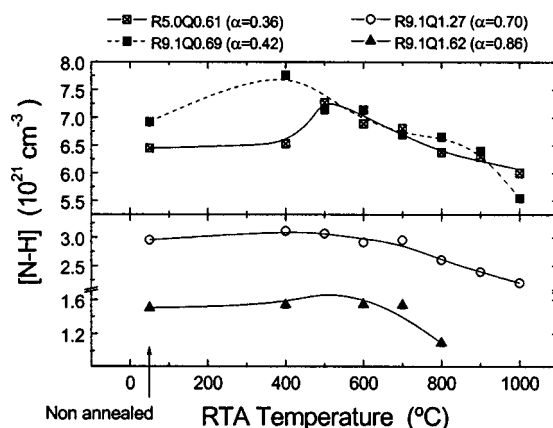


FIG. 4. N–H bond concentration as a function of the RTA temperature for samples deposited at $R=5.0$ and 9.1 and different values of Q . The lines are a guide to the eye.

TABLE I. Relative loss of H after RTA at $T=1000^\circ\text{C}$.

Sample	$\alpha=2x/(2x+3y)$	ΔH_0 (%)	ΔH_{\max} (%)
R1.6Q0	0	60	80
R1.6Q.21	0.13	35	48
R1.6Q0.53	0.34	48	52
R1.6Q0.80	0.53	62	62
R5.0Q0.61	0.36	7	17
R9.1Q0.69	0.42	20	29
R9.1Q1.27	0.70	25	29

For intermediate compositions (samples R5.0Q0.61 with $\alpha=0.36$ and R9.1Q0.69 with $\alpha=0.42$), a clear increase of N–H bond concentration is observed for low annealing temperatures ($T=400\text{--}500^\circ\text{C}$). For higher annealing temperatures the N–H concentration decreases with respect to the maximum value and below the concentration of the nonannealed samples for $T=700\text{--}800^\circ\text{C}$. On the other hand, for the samples with composition closer to SiO_2 (R9.1Q1.27 with $\alpha=0.70$ and R9.1Q1.62 with $\alpha=0.86$), the N–H bond concentration remains roughly constant for annealing temperatures up to 700°C and decreases for $T=800^\circ\text{C}$ and higher.

It must be noted that the relative decrease of the N–H concentration of the samples with no Si–H bonds (series R5.0 and R9.1, Fig. 4) is much lower than in those with both Si–H and N–H bonds (series R1.6, Fig. 3). The total (Si–H + N–H) relative H loss for the different samples is summarized in Table I. Two values are given: ΔH_0 which is the relative H loss after the annealing at $T=1000^\circ\text{C}$ with respect to the nonannealed sample, and ΔH_{\max} , which is the relative loss with respect to the maximum H concentration.

Another important parameter for Si–H and N–H stretching bands is the wave number of the maximum of the band. It is known that, as the combined electronegativity of the first neighbors of the Si atom in the Si–H bond increases, the wave number of the band shifts towards higher wave numbers; from $\nu_{\text{SiH}}=2000\text{ cm}^{-1}$ for the $(\text{Si}_3)\text{--Si--H}$ configuration (lowest electronegativity)^{30,31} to $\nu_{\text{SiH}}=2245\text{--}2265\text{ cm}^{-1}$ for $(\text{O}_3)\text{--Si--H}$ (highest electronegativity).^{30,31} A shift of the N–H band towards higher wave numbers as the composition changes from silicon nitride to silicon oxide in $\text{SiO}_x\text{N}_y\text{H}_z$ films has also been reported.^{4,11} So, the study of these bands provides qualitative information concerning bonding rearrangement within the lattice.

Figure 5 shows the wave number of the maximum of the Si–H stretching band (ν_{SiH}) as a function of the annealing temperature for samples deposited at $R=1.6$ and different values of Q . For the silicon nitride sample (R1.6Q0, $\alpha=0$) the value of the nonannealed sample ($\nu_{\text{SiH}}=2226\text{ cm}^{-1}$) remains unaffected for temperatures up to 500°C . For higher annealing temperatures the band shifts towards lower wave numbers, especially for $T>700^\circ\text{C}$, with a total shift of $\Delta\nu_{\text{SiH}}=46\text{ cm}^{-1}$ for $T=1000^\circ\text{C}$. The behavior of sample R1.6Q0 ($\alpha=0.13$), with composition close to that of nitride, is similar, but the shift towards lower wave numbers begins

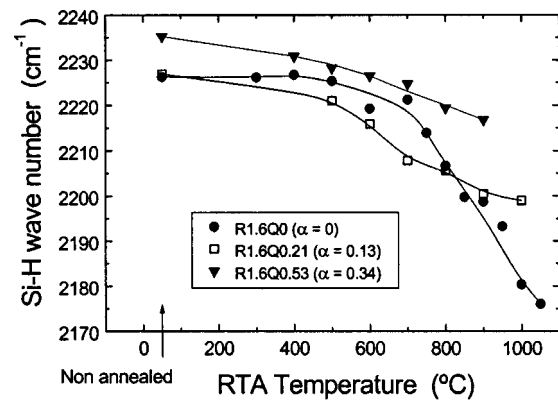


FIG. 5. Wave number of the maximum of the Si–H stretching band as a function of the RTA temperature for samples deposited at $R=1.6$ and different values of Q . The lines are a guide to the eye.

at lower temperatures and is less significant ($\Delta\nu_{\text{SiH}}=28\text{ cm}^{-1}$). For sample R1.6Q0.53 ($\alpha=0.34$) the Si–H band continuously shifts towards lower wave numbers over the whole temperature range, with a total shift of $\Delta\nu_{\text{SiH}}=19\text{ cm}^{-1}$.

With respect to the wave number of the maximum of the N–H band, for $\text{SiO}_x\text{N}_y\text{H}_z$ samples no significant change is observed in the temperature range studied ($T=400\text{--}1000^\circ\text{C}$).

In addition to the bands related to H bonds, in $\text{SiO}_x\text{N}_y\text{H}_z$ samples the FTIR spectrum shows very intense bands that correspond to Si–N and Si–O stretching oscillations. For homogeneous films (ones with no phase separation) a single Si–O/Si–N band is observed. This band appears at intermediate wave numbers between the characteristic values of silicon nitride and silicon oxide (860 and 1070 cm^{-1} , respectively),^{32,33} depending on the composition.^{1,4–6,10,11} However, for a given composition, the exact wave number of the band may be affected by other factors, such as mechanical stress.¹³

The samples studied in this work are essentially single phase, and show a single Si–O/Si–N band.²⁸ No significant changes in the wave number of the maximum of this band are observed after RTA for compositions in the range of $\alpha=0\text{--}0.6$. This behavior is shown in Fig. 6. On the other hand, for compositions closer to that of silicon oxide ($\alpha>0.6$) a shift of the band towards higher wave numbers is observed for annealing temperatures above 600°C , as shown in Fig. 7.

The full width at half maximum (FWHM) of the Si–O/Si–N band is also a very useful parameter since it is related to structural order of the film, with a higher FWHM for higher dispersion of different chemical environments (and therefore higher disorder).^{34,35} The behavior of the FWHM of the Si–O/Si–N band as a function of the RTA temperature for samples of different composition is shown in Fig. 8 (samples of series R1.6) and Fig. 9 (samples of series R5.0 and R9.1).

For the samples deposited at $R=1.6$, with both Si–H and N–H bonds (Fig. 8), the FWHM increases for annealing temperatures above 600°C , suggesting degradation of the

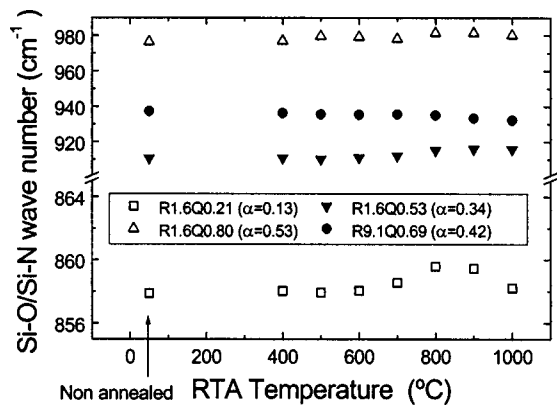


FIG. 6. Wave number of the maximum of Si-O/Si-N stretching band as a function of the RTA temperature for samples with composition in the $\alpha=0-0.60$ range.

structural order. On the other hand, for the samples deposited at $R=5.0$ and 9.1 , with N-H bonds only (Fig. 9), the FWHM decreases for annealing temperatures above 700°C . So, for these samples the RTA improves the structural order. Note the different behavior of samples with similar values of α (samples R1.6Q0.53 with $\alpha=0.34$ and R5.0Q0.61 with $\alpha=0.36$), depending on the value of R , i.e., it depends on the presence of both Si-H and N-H bonds ($R=1.6$) or N-H bonds only ($R=5.0$).

Finally, the influence of RTA on the absorption area of the Si-O/Si-N band was also investigated. While calculation of the Si-N and Si-O bond concentrations in this area is not as straightforward as in the case of Si-H and N-H bands, for a given composition it provides qualitative information about possible formation or breaking of these bonds during the RTA process.^{12,21}

The normalized area of the Si-O/Si-N stretching band (area/thickness) as a function of the RTA temperature is shown in Figs. 10 and 11 for samples of different composition. As in the case of the FWHM, the behavior of the samples deposited at $R=1.6$ (Fig. 10), with both Si-H and N-H bonds, is different than the behavior of samples deposited at $R=5.0$ and 9.1 (Fig. 11), with N-H bonds only. For the samples deposited at $R=1.6$, an increase of the area is

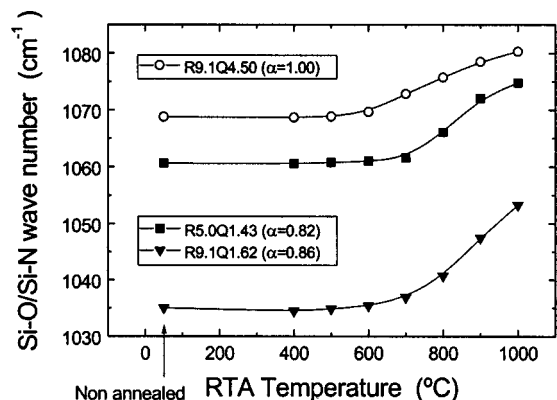


FIG. 7. Wave number of the maximum of the Si-O/Si-N stretching band as a function of the RTA temperature for samples with composition in the $\alpha=0.60-1.00$ range. The lines are a guide to the eye.

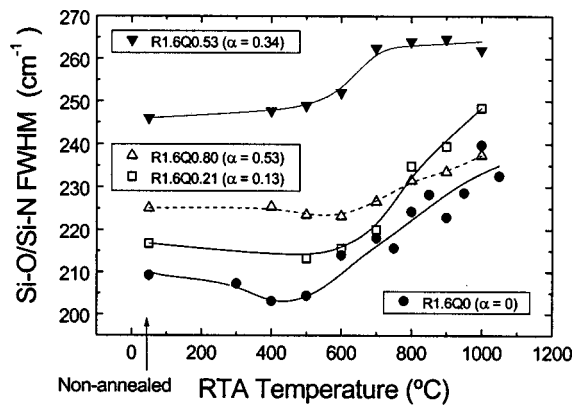


FIG. 8. FWHM of the Si-O/Si-N stretching band as a function of the RTA temperature for samples deposited at $R=1.6$ and different values of Q . The lines are a guide to the eye.

observed in the $600-700^\circ\text{C}$ temperature range. For higher temperatures the area of the band decreases, especially for samples with composition closer to that of SiN_yH_z . On the other hand, for the samples deposited at $R=5.0$ and 9.1 no significant changes in band area are observed for any composition, suggesting that RTA of these samples does not result in the formation or breaking of Si-N and Si-O bonds. Note that behavior in the area of the Si-O/Si-N band shown in Figs. 10 and 11 is not correlated with the behavior of the FWHM (Figs. 8 and 9). So, the changes in the band area cannot be explained just by a change in shape due to the increase or decrease of the FWHM of the band, and the formation or breaking of Si-O and/or Si-N bonds is very likely involved.

C. EPR

The most important paramagnetic defects detected in our samples are the well-known Si dangling bonds; basically the K center ($\text{N}_3\equiv\text{Si}\uparrow$) and the E' center ($\text{O}_3\equiv\text{Si}\uparrow$), with some variants, such as $\text{SiN}_2\equiv\text{Si}\uparrow$, $\text{Si}_2\text{N}\equiv\text{Si}\uparrow$, $\text{Si}_3\equiv\text{Si}\uparrow$ (this last is also known as the D center),⁵ $\text{SiO}_2\equiv\text{Si}\uparrow$ or $\text{O}_2\text{H}\equiv\text{Si}\uparrow$. A detailed study of the EPR spectrum of our $\text{SiO}_x\text{N}_y\text{H}_z$ films was presented in a previous paper.²⁸

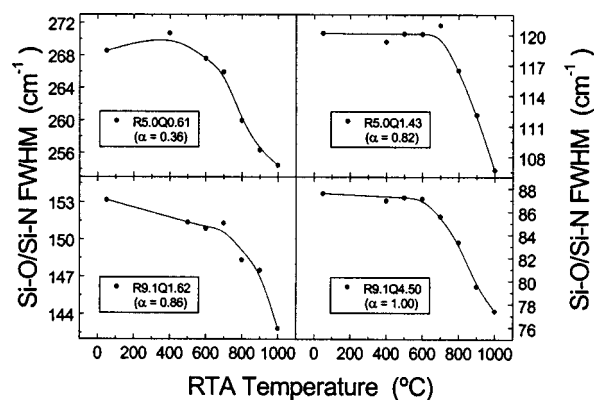


FIG. 9. FWHM of the Si-O/Si-N stretching band as a function of the RTA temperature for samples deposited at $R=5.0$ and 9.1 and different values of Q . The lines are a guide to the eye.

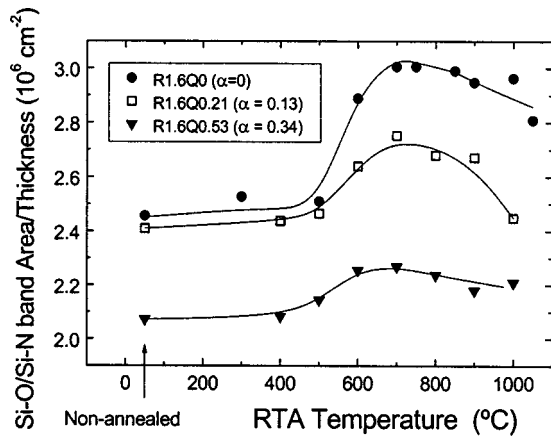


FIG. 10. Normalized area (area/thickness) of the Si-O/Si-N band as a function of the RTA temperature for samples deposited at $R=1.6$ and different values of Q . The lines are a guide to the eye.

Figure 12 shows the overall density of paramagnetic defects N_D (K center + E' center + their variants) as a function of the RTA temperature for representative samples deposited at different values of R and Q . For the samples deposited at $R=1.6$ (shown in the upper part of the graph) a minimum of N_D is observed for $T=500-600$ °C, and for higher annealing temperatures N_D increases but remains below the value for the nonannealed sample. For SiO_2 films (sample R9.1Q4.5, $\alpha=1$), the density of defects remains low over the whole annealing temperature range, with a minimum value for $T=300-400$ °C. For sample R5.0Q1.43, with composition close to that of silicon oxide ($\alpha=0.82$), N_D decreases up to annealing temperatures of 700 °C and then increases, in a way similar to the samples deposited at $R=1.6$. Finally, the behavior of sample R5.0Q0.61 ($\alpha=0.36$) is similar to that of sample R5.0Q1.43, but for $T>700$ °C the density of defects remains roughly constant at the minimum value rather than increasing.

For most samples the defects detected are the same over the whole RTA temperature range. However, for $\text{SiO}_x\text{N}_y\text{H}_z$ films with composition very close to that of SiO_2 (sample R5.0Q1.43, $\alpha=0.82$) the shape of the EPR spectrum is

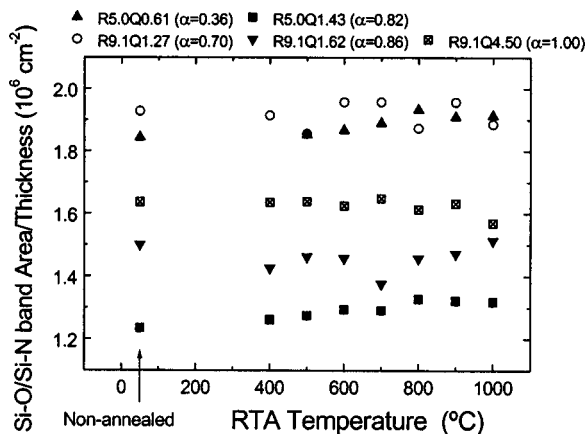


FIG. 11. Normalized area (area/thickness) of the Si-O/Si-N band as a function of the RTA temperature for samples deposited at $R=5.0$ and 9.1 and different values of Q .

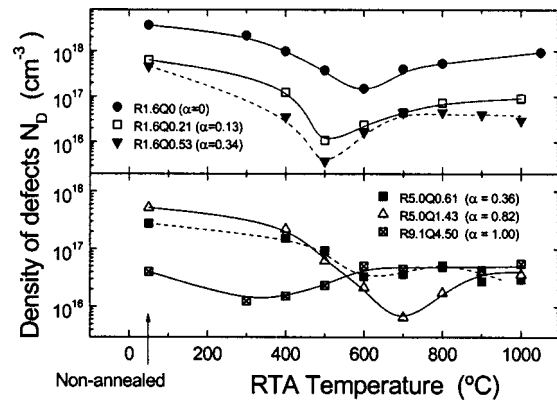


FIG. 12. Overall density of paramagnetic defects (N_D) as a function of the RTA temperature for samples of different compositions. The lines are a guide to the eye.

strongly affected, as shown in Fig. 13. The spectrum of the nonannealed sample is discussed in detail elsewhere.²⁸ Three different signals are detected: an intense feature located at $g=2.0008$, attributed to an E' -like center typical of silicon suboxide films ($\text{SiO}_2\equiv\text{Si}\uparrow$);³⁶ a 73 G doublet, attributed to a variant of the E' center ($\text{O}_2\text{H}\equiv\text{Si}\uparrow$);³⁷ and a 22 G doublet which was tentatively attributed to the N_4^0 center.³⁸ As the annealing temperature increases these signals strongly decrease, and a signal located around $g=2.005$ becomes apparent. This value is close to the characteristic value of the D center ($\text{Si}_3\equiv\text{Si}\uparrow$, $g=2.0055$),⁵ and therefore we attribute this signal to this defect.

D. Ellipsometry

By ellipsometry measurement the refractive index and thickness of the films can be calculated. The results for some characteristic samples are shown in Fig. 14. Some authors have reported modifications in the refractive index of SiO_2 ,¹³ SiN_yH_z ,³⁹ and $\text{SiO}_x\text{N}_y\text{H}_z$ films.⁴⁰ These modifications are correlated to changes in the density of the films. For SiN_yH_z films deposited at $R=1.6$, a slight decrease of refractive index was observed by our group for high annealing temperatures ($T>900$ °C).¹⁸ This decrease was related to N release.

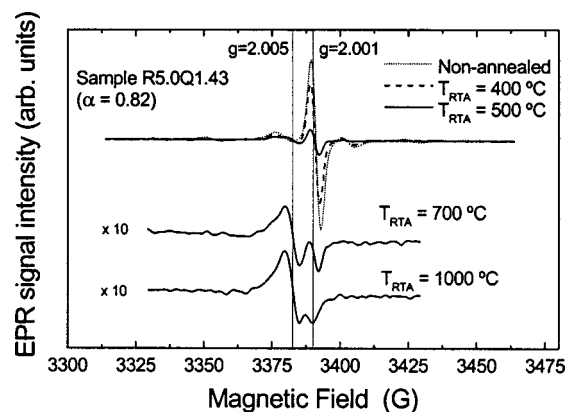


FIG. 13. EPR spectra of sample R5.0Q1.43 ($\alpha=0.82$) for different RTA temperatures.

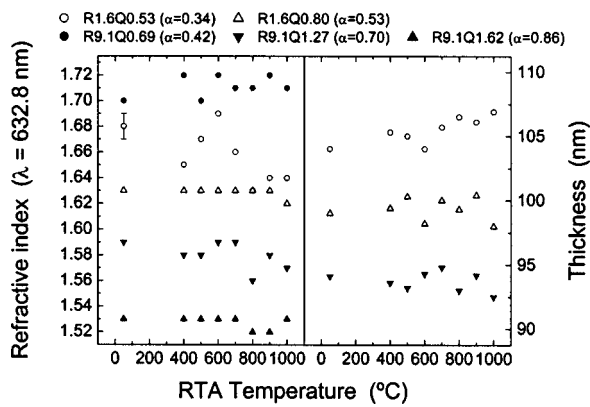


FIG. 14. Refractive index for $\lambda=632.8$ nm (left) and thickness (right), determined by ellipsometry, as a function of the RTA temperature for samples of different compositions.

As shown in Fig. 14, no significant changes in the refractive index or in the thickness of the films are observed for most $\text{SiO}_x\text{N}_y\text{H}_z$ and SiO_2 . Only for sample R1.6Q0.53 ($\alpha=0.34$) is there a trend for the refractive index to decrease. However, this decrease is of the same order as dispersion of the measurements so no definitive conclusions can be reached.

IV. DISCUSSION

A. $\text{SiO}_x\text{N}_y\text{H}_z$ films with composition close to that of SiO_2

We will start by discussing the behavior of samples with composition close to that of SiO_2 , i.e., samples with values of α close to 1. The composition limit for what can be understood as “close to SiO_2 ” is not evident. As shown in Sec. III, H release is one important effect of the RTA process (Figs. 2–4) and the H content in our nonannealed $\text{SiO}_x\text{N}_y\text{H}_z$ films significantly decreases as composition parameter α increases (Figs. 2–4). So, it seems convenient to consider as close to SiO_2 composition those films in which the H concentration is very low or even below the limit of detection. Therefore we will include in this group those films with $\alpha > 0.8$. In these samples the H concentration is in the low 10^{21} cm^{-3} range or lower (see sample R9.1Q1.62 with $\alpha=0.86$ in Fig. 4).

For SiO_2 films, with negligible H content, thermal relaxation of the lattice was reported by our group.²³ This thermal relaxation was evidenced mainly by two results. First, the wave number of the Si–O stretching vibration shifts towards higher values for annealing temperatures above 600 °C. This is reproduced in Fig. 7 (sample R9.1Q4.50, $\alpha=1.00$). According to the center force model, the wave number of the Si–O band (ν_{SiO}) is given by¹³

$$\nu_{\text{SiO}} = \nu_0 \sin \theta, \quad (1)$$

where θ is half the Si–O–Si bond angle and ν_0 is an empirical constant: $\nu_0 = 1134 \text{ cm}^{-1}$. The bond angle is directly related to the distance between the Si atoms $d_{\text{Si-Si}}$:¹³

$$d_{\text{Si-Si}} = 2r_0 \sin \theta, \quad (2)$$

where r_0 is the Si–O bond length.

The $d_{\text{Si-Si}}$ distance depends on the mechanical stress of the films, so when the stress decreases, $d_{\text{Si-Si}}$ increases and so too do angle θ and the wave number of the Si–O band ν_{SiO} .¹³ Therefore, the observed increase of the Si–O stretching band wave number shown in Fig. 7 for sample R9.1Q4.50 ($\alpha=1.00$) is due to thermal relaxation of the lattice accompanied by a decrease of mechanical stress.

This thermal relaxation is also evidenced by the decrease of the FWHM of the band in the same RTA temperature range (Fig. 9), which is understood as improvement of the structural order of the films. As shown in Figs. 7 and 9, the behavior of $\text{SiO}_x\text{N}_y\text{H}_z$ samples with composition close to that of SiO_2 ($\alpha > 0.8$) is essentially the same as that described for SiO_2 . Because the H content in these films is very low, no significant effect associated to H release during RTA is observed. So, it is concluded that the main effect of RTA on the structural properties of $\text{SiO}_x\text{N}_y\text{H}_z$ films with composition close to that of SiO_2 is thermal relaxation of the lattice.

With respect to the density of paramagnetic defects (N_D) for SiO_2 films (sample R9.1Q4.50, with $\alpha=1.00$ in Fig. 12), the only defect detected is the E' center. Over the whole annealing temperature range N_D remains at a low value, with a minimum at $T=300\text{--}400$ °C. This minimum may be related to the passivation of defects by nonbonded H present in the films.²³

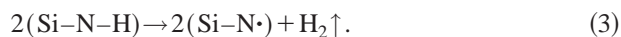
The behavior of $\text{SiO}_x\text{N}_y\text{H}_z$ samples with composition close to that of SiO_2 (sample R5.0Q1.43, with $\alpha=0.82$ in Figs. 12 and 13) is more complex. For the nonannealed sample, the EPR signal is mainly due to an E' -like defect ($\text{SiO}_2 \equiv \text{Si}\uparrow$), with $g=2.0008$, as explained in Sec. III. The intensity of this signal decreases as the RTA temperature is increased up to $T=1000$ °C. However, for $T=700$ °C a weak signal located around $g=2.005$ (the D center, previously discussed) can be distinguished and it becomes more intense for higher annealing temperatures, and is responsible for the increase of the overall density of paramagnetic defects shown in Fig. 12. Very similar behavior was observed by our group for silicon suboxide films, SiO_xH_z ($x \approx 1.9$).²⁴ For these SiO_xH_z films the density of E' centers also decreases over the whole RTA temperature range up to $T=1000$ °C, while the density of D centers increases for temperatures above 700 °C. This result was attributed to a network reaction in which high quality SiO_2 formed together with highly defective Si clusters. It is tentatively suggested that a process similar to that observed for silicon suboxide may also take place in $\text{SiO}_x\text{N}_y\text{H}_z$ films with composition close to that of silicon oxide (sample R5.0Q1.43, with $\alpha=0.82$).

B. $\text{SiO}_x\text{N}_y\text{H}_z$ films deposited at $R=5.0$ and 9.1 (with N–H bonds only)

As previously shown, H is present in our $\text{SiO}_x\text{N}_y\text{H}_z$ films in the form of Si–H and N–H bonds. Additionally, in previous work the incorporation of H into our $\text{SiO}_x\text{N}_y\text{H}_z$ films was studied in detail using heavy ion-elastic recoil detection analysis (HI-ERDA) and FTIR measurements.⁴¹ In this work it was concluded that H in a nonbonded state was present in the films, and was also present in higher concen-

trations for compositions close to that of SiN_yH_z . We will now consider those films deposited at $R=5.0$ and 9.1 , in which a significant concentration of N–H bonds is detected, but the Si–H bond concentration is negligible.

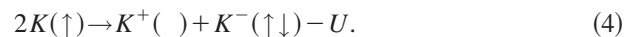
For samples R5.0Q0.61 ($\alpha=0.36$) and R9.1Q0.69 ($\alpha=0.42$), an increase of the N–H concentration is observed for $T=400\text{--}500^\circ\text{C}$ (see Fig. 4). This increase is attributed to the formation of new bonds at the expense of nonbonded H present in the films. This mechanism is not clearly observed in films with compositions closer to that of SiO_2 (samples R9.1Q1.27, with $\alpha=0.70$ and R9.1Q1.62, with $\alpha=0.86$), which is due to the lower concentration of nonbonded H as the composition nears that of SiO_2 .⁴¹ For higher annealing temperatures ($T=600\text{--}700^\circ\text{C}$) the N–H concentration decreases with respect to the maximum value, suggesting that nonbonded H may be released and that the formation of N–H bonds is significantly reduced. Finally, for annealing temperatures about of $T=800^\circ\text{C}$ and higher, the N–H concentration decreases below the value of that of the nonannealed sample. We propose that the mechanism for the release of bonded H in these films is the direct breaking of N–H bonds:



Reaction (3) is consistent with the behavior of the area of the Si–N/Si–O stretching band in these samples (Fig. 11), with no significant change over the whole annealing temperature range, since it does not imply the formation or breaking of Si–N or Si–O bonds.

The FWHM of the Si–O/Si–N stretching band also decreases for annealing temperatures above 600°C , like in the case of $\text{SiO}_x\text{N}_y\text{H}_z$ films with composition close to that of SiO_2 (sample R5.0Q0.61, with $\alpha=0.36$, in Fig. 9). In previous work we also observed a decrease of the FWHM of the Si–N stretching band of SiN_yH_z films deposited at $R=7.5$ (with N–H bonds only) for annealing temperatures up to 900°C , and an increase with respect to the minimum for higher annealing temperatures, coincident with the release of H.^{21,23} As previously explained, the decrease of the FWHM is associated with improvement of the structural order as a result of thermal relaxation of the lattice induced by RTA. However, the release of H results in degradation of the structural order and a subsequent increase of the FWHM. In the $\text{SiO}_x\text{N}_y\text{H}_z$ films deposited at $R=5.0$ and 9.1 the loss of H after RTA at $T=1000^\circ\text{C}$ is relatively low, less than 30% with respect to the maximum value (see Table I). Therefore degradation of the structural order associated with H release is not critical and the thermal relaxation process prevails up to $T=1000^\circ\text{C}$, so the FWHM decreases as shown in Fig. 9.

The behavior of the density of paramagnetic defects (N_D) for sample R5.0Q0.61, with $\alpha=0.36$, is shown in Fig. 12 as an example of the behavior of $\text{SiO}_x\text{N}_y\text{H}_z$ films with N–H bonds only. The decrease of N_D for RTA temperatures up to 600°C is attributed to two possible mechanisms: First, the passivation of defects at the expense of the nonbonded H, and, second, charge transfer between the neutral paramagnetic states of the K center and the charged diamagnetic ones:



This charge transfer is very likely, since the correlation energy U is negative (negatively charged states are more stable).⁴² In previous work we discussed in detail this mechanism in SiN_yH_z films.¹⁹

C. $\text{SiO}_x\text{N}_y\text{H}_z$ films deposited at $R=1.6$ (with both Si–H and N–H bonds)

We now will discuss RTA effects on $\text{SiO}_x\text{N}_y\text{H}_z$ films deposited at $R=1.6$, which contain both Si–H and N–H bonds.

For SiN_yH_z films deposited at $R=1.6$ the concentration of both Si–H and N–H bonds increases for low annealing temperatures (sample R1.6Q0, with $\alpha=0$, in Figs. 2 and 3). The same behavior is observed for $\text{SiO}_x\text{N}_y\text{H}_z$ films with composition close to that of SiN_yH_z (sample R1.6Q0.21, with $\alpha=0.13$). As previously explained, this increase of the bonded H content is attributed to the formation of new Si–H and N–H bonds at the expense of the nonbonded H in the films. However, while the maximum N–H concentration is achieved for annealing temperatures in the $400\text{--}500^\circ\text{C}$ range, the Si–H concentration increases for T up to 700°C , suggesting a different or an additional mechanism for the formation of Si–H bonds.

For SiN_yH_z films we explained this behavior by the well-known interchange network reaction,²¹



in which Si–H and Si–N bonds form at the expense of Si–Si and N–H bonds. The fact that reaction (5) takes place is supported by the increase of the area of the Si–N absorption band for annealing temperatures up to 700°C (Fig. 10).

Because the behavior of $\text{SiO}_x\text{N}_y\text{H}_z$ films with composition close to that of silicon nitride (sample R1.6Q0.21, with $\alpha=0.13$) is essentially the same as that of SiN_yH_z films, we propose that reaction (4) also takes place for $\text{SiO}_x\text{N}_y\text{H}_z$ films of near-nitride composition.

Note that reaction (5) requires the presence of both Si–Si and N–H bonds. In our samples the Si content is controlled by parameter R , so Si-rich films are obtained for low values of R .^{21,28} Excess Si is evidenced by the presence of Si–H bonds. In this work, reaction (5) is expected to take place only in those samples that show both Si–H and N–H bonds (samples deposited at $R=1.6$). Note that in the films deposited at $R=5.0$ and 9.1 , with N–H bonds only, reaction (5) does not take place and, therefore, no increase of the Si–O/Si–N stretching band area associated with the formation of Si–N bonds is observed (Fig. 11).

Additionally, for nonannealed samples, as the composition changes from silicon nitride to silicon oxide, the concentration of N–H bonds decreases, due to a decrease of the N content, and the Si–H concentration due to the substitution of Si–H bonds by Si–O bonds also decreases.¹¹ The decrease of the Si–H concentration is an indication that the Si–Si bond concentration also decreases. So, for the samples deposited at $R=1.6$, as parameter Q is increased (and therefore composition parameter α), reaction (5) is less likely to occur. This is evidenced by a lower increase of the Si–H bond

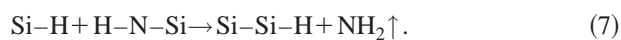
concentration, which is almost negligible for sample R1.6Q0.53, with $\alpha=0.34$, (Fig. 2), and also by a lower increase of the Si–O/Si–N band area (Fig. 10).

For the samples deposited at $R=1.6$, with both Si–H and N–H bonds, the release of H at high annealing temperatures is also observed. As shown in Table I, this H release is more significant than in samples containing N–H bonds only. The same trend was reported by Denisse *et al.*⁴³ In fact, for SiN_yH_z films, we calculated the activation energies (E_a) for the process of H release, and found $E_a=1.22$ eV for samples deposited at $R=1.6$ (with both Si–H and N–H bonds) and $E_a=2.00$ eV for samples deposited at $R=7.5$ (with N–H bonds only).²¹ This behavior is due to cooperative reactions between Si–H and N–H bonds that take place in the network. Lu *et al.* proposed the following reaction for SiN_yH_z films:¹²



This is the same reaction suggested by Denisse *et al.* for $\text{SiO}_x\text{N}_y\text{H}_z$ films.⁴³ It must be noted that reaction (6) implies the formation of Si–N bonds, and is accompanied by enhancement of the Si–N absorption band.¹² As shown in Fig. 10, in our samples containing both Si–H and N–H bonds ($R=1.6$), for high RTA temperatures at which the H content decreases, the Si–O/Si–N band has a tendency to decrease, in contrast to the increase predicted by reaction (6). So, it is concluded that this reaction does not take place in our samples.

Moreover, we observed a decrease of N content in SiN_yH_z films, which suggests a reaction in which N is released together with H. The following reaction was proposed by our group for SiN_yH_z films:²¹



The ammonia fragment, NH_2 , is able to later capture an additional H atom and form an ammonia molecule.

The behavior of the wave number of the maximum of the Si–H band (Fig. 5) further supports this reaction. If the Si atom bonded to the N–H group is also part of a Si–H bond, reaction (7) results in the replacement of a N atom in the chemical environment of the Si–H bond by a Si atom (with lower electronegativity), with a subsequent decrease of the frequency of Si–H oscillation.^{21,30}

For $\text{SiO}_x\text{N}_y\text{H}_z$ films reaction (7) may also take place during RTA, especially for compositions close to that of silicon nitride. However, as composition parameter α increases, the lower Si–H bond concentration makes it less likely. In fact, for sample R1.6Q0.53, with $\alpha=0.34$, no significant change in composition was observed (Fig. 1). At this composition the N loss may be too small to be resolved by AES measurements. Note also that the decrease of the Si–O/Si–N band area in this sample for high annealing temperatures (Fig. 10) and the shift towards lower wave numbers of the Si–H stretching band (Fig. 5) are much lower than in samples R1.6Q0, with $\alpha=0$, and R1.6Q0.21, with $\alpha=0.13$.

In the films deposited at $R=1.6$, with Si–H and N–H bonds, breaking of N–H bonds [reaction (3)] is also possible.

This reaction becomes more significant with respect to H release in those samples with low Si–H concentrations, in which reaction (7) is less likely.

Note that reactions (3), (5) and (7), which we propose as an explanation of H release during RTA in our $\text{SiO}_x\text{N}_y\text{H}_z$ films, do not involve O atoms directly (although O atoms may be bonded to the Si atoms in these reactions). This is due to two facts. First, no O–H bonds were detected in our samples, so they were not considered in the discussion. Second, the presence of H in our samples is correlated to the concentration of N. While the N–H bond concentration is proportional to the N content,⁴¹ the same direct relationship cannot be applied to Si–H bonds and Si. Although the presence of Si–H bonds is related to the presence of excess Si, for a given value of R the Si–H concentration decreases as the composition nears that of silicon oxide. In fact, for silicon nitride samples deposited at $R=1.6$ Si–H bonds are detected, but for silicon oxide deposited at the same $R=1.6$ value, the Si–H bond concentration is below the limit of detection, as shown in previous work.⁴⁴ This is due to the fact that O_2 is more reactive than N_2 .¹¹ So, the reactions that involve H imply Si and N, but not O atoms in a direct way.

With respect to the structural order of the samples, the FWHM of the Si–O/Si–N stretching band increases for annealing temperatures above 600 °C in the samples deposited at $R=1.6$, with both Si–H and N–H bonds (see Fig. 8), especially for the SiN_yH_z (sample R1.6Q0, with $\alpha=0$) and $\text{SiO}_x\text{N}_y\text{H}_z$ films of near-nitride composition (sample R1.6Q0.21, with $\alpha=0.13$). This behavior is opposite that described in Sec. IV B for the films deposited at $R=5.0$ and 9.1, with N–H bonds only. While the thermal relaxation process also takes place in the films deposited at $R=1.6$, the H release process is more significant due to the cooperative reaction between Si–H and N–H bonds [reaction (7)], as shown in Table I. So, in these samples degradation of the structural order associated with H release prevails over the thermal relaxation process. The N loss which accompanies H release in SiN_yH_z films (sample R1.6Q0) and in near compositions (sample R1.6Q0.21) enhances the degradation of structural order.

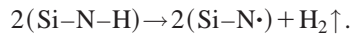
Finally, we will discuss the influence of RTA on the density of paramagnetic defects (N_D) of the samples deposited at $R=1.6$ (Fig. 12, upper part of the graph). The decrease of N_D observed for annealing temperatures up to 500–600 °C is explained by the same mechanisms described in Sec. IV B: the passivation of bonds by the nonbonded H present in the films, and the transition from the paramagnetic state to the diamagnetic state of the K center. However, unlike in the case of sample R5.0Q0.61, for higher annealing temperatures, the density of paramagnetic defects of the films deposited at $R=1.6$ (with Si–H and N–H bonds) increases with respect to the minimum. This increase is attributed to the H release that takes place in these samples, which is more significant than in samples deposited at $R=5.0$ and 9.1 (with N–H bonds only).

V. CONCLUSIONS

The influence of RTA processes on the structural properties of $\text{SiO}_x\text{N}_y\text{H}_z$ films was analyzed. Different mechanisms are activated by RTA depending on the composition of the samples.

For SiO_2 films and $\text{SiO}_x\text{N}_y\text{H}_z$ films of composition close to that of SiO_2 (about $\alpha > 0.8$), which have a very low or negligible H content, the main effect of RTA on the structural properties is thermal relaxation of the lattice.

For $\text{SiO}_x\text{N}_y\text{H}_z$ samples deposited at $R=5.0$ and 9.1 , which contain N–H bonds but no significant concentration of Si–H bonds, H is released at high annealing temperatures ($T=800^\circ\text{C}$ and higher) due to the breaking of N–H bonds, described by reaction (3)



In these samples, the density of paramagnetic defects decreases for annealing temperatures up to 600°C due to the passivation of defects by nonbonded H in the films and the transition from the paramagnetic to the more stable diamagnetic state of the K center.

For samples deposited at relatively high SiH_4 partial pressure ($R=1.6$), in which both Si–H and N–H bonds are present, a transfer reaction between N–H and Si–H was observed for RTA temperatures up to 700°C :



As the composition changes from SiN_yH_z to SiO_2 (α increases), this reaction is less likely to take place because of the decrease of the concentration of Si–Si bonds. This reaction was not observed for samples deposited at $R=5.0$ and 9.1 .

For high annealing temperatures ($T > 700^\circ\text{C}$) a cooperative reaction between Si–H and N–H bonds enhances the H release process:



This reaction is less likely to happen as the composition parameter α is increased.

The H release is more significant in the films deposited at $R=1.6$ (with Si–H and N–H bonds) than in the films deposited at $R=5.0$ and 9.1 (with N–H bonds only). Thus, the degradation of structural order associated with H release prevails over thermal relaxation in the films deposited at $R=1.6$. On the other hand, in the films deposited at $R=5.0$ and 9.1 , thermal relaxation of the lattice prevails over H release.

In the samples deposited at $R=1.6$, minimum density of paramagnetic defects (N_D) is achieved for $T=500\text{--}600^\circ\text{C}$. For higher annealing temperatures N_D increases as a consequence of the release of H.

ACKNOWLEDGMENTS

The authors acknowledge Centro de Asistencia a la Investigación (CAI) de Implantación Iónica [Universidad Complutense de Madrid (UCM)] for use of the deposition system and RTA furnace. CAI de Espectroscopia (UCM) is

acknowledged for providing the FTIR spectrometer. This work was partially financed by the CICYT (Spain) under Contract No. TIC 01-1253.

- ¹S. V. Hattangady, H. Niimi, and G. Lucovsky, *J. Vac. Sci. Technol. A* **14**, 3017 (1996).
- ²M. M. Moslehi, R. A. Chapman, M. Wong, A. Paranjpe, H. N. Najm, J. Kuehne, R. L. Yeakley, and C. J. Davis, *IEEE Trans. Electron Devices* **39**, 4 (1992).
- ³W. A. P. Claassen, H. A. J. Th. v. d. Pol, A. H. Goemans, and A. E. T. Kuiper, *J. Electrochem. Soc.* **133**, 1458 (1986).
- ⁴C. M. M. Denisse, K. Z. Troost, J. B. Oude Elferink, F. H. P. M. Habraken, W. F. van der Weg, and M. Hendriks, *J. Appl. Phys.* **60**, 2536 (1986).
- ⁵L.-N. He, T. Inokuma, and S. Hasegawa, *Jpn. J. Appl. Phys., Part 1* **35**, 1503 (1996).
- ⁶Y. Ma and G. Lucovsky, *J. Vac. Sci. Technol. B* **12**, 2504 (1994).
- ⁷M. Hernández Vélez, O. Sánchez Garrido, F. Fernández Gutiérrez, C. Falcony, and J. M. Martínez-Duart, *J. Vac. Sci. Technol. B* **16**, 1087 (1998).
- ⁸P. V. Bulkin, P. L. Swart, and B. M. Lacquet, *J. Non-Cryst. Solids* **187**, 484 (1995).
- ⁹D. Landheer, Y. Tao, J. E. Hulse, T. Quance, and D.-X. Xu, *J. Electrochem. Soc.* **143**, 1681 (1996).
- ¹⁰M. J. Hernández, J. Garrido, J. Martínez, and J. Piqueras, *Semicond. Sci. Technol.* **12**, 927 (1997).
- ¹¹A. del Prado, I. Mártil, M. Fernández, and G. González-Díaz, *Thin Solid Films* **343–344**, 432 (1999).
- ¹²Z. Lu, P. Santos-Filho, G. Stevens, M. J. Williams, and G. Lucovsky, *J. Vac. Sci. Technol. A* **13**, 607 (1995).
- ¹³J. T. Fitch, S. S. Kim, and G. Lucovsky, *J. Vac. Sci. Technol. A* **8**, 1871 (1990).
- ¹⁴Y. Ma, T. Yasuda, and G. Lucovsky, *J. Vac. Sci. Technol. B* **11**, 1533 (1993).
- ¹⁵W. K. Choi, C. K. Choo, and Y. F. Lu, *J. Appl. Phys.* **80**, 5837 (1996).
- ¹⁶D. Landheer, J. E. Hulse, and T. Quance, *Thin Solid Films* **293**, 52 (1997).
- ¹⁷N. Bhat, A. W. Wang, and K. C. Sarawat, *IEEE Trans. Electron Devices* **46**, 63 (1999).
- ¹⁸F. L. Martínez, A. del Prado, I. Mártil, G. González-Díaz, B. Selle, and I. Sieber, *J. Appl. Phys.* **86**, 2055 (1999).
- ¹⁹F. L. Martínez, A. del Prado, I. Mártil, D. Bravo, and F. J. López, *J. Appl. Phys.* **88**, 2149 (2000).
- ²⁰F. L. Martínez, E. San Andrés, A. del Prado, I. Mártil, D. Bravo, and F. J. López, *J. Appl. Phys.* **90**, 1573 (2001).
- ²¹F. L. Martínez, A. del Prado, I. Mártil, G. González-Díaz, W. Bohne, W. Fuhs, J. Röhrich, B. Selle, and I. Sieber, *Phys. Rev. B* **63**, 245320 (2001).
- ²²F. L. Martínez, A. del Prado, I. Mártil, G. González-Díaz, K. Kliefoth, and W. Füssel, *Semicond. Sci. Technol.* **16**, 534 (2001).
- ²³E. San Andrés, A. del Prado, F. L. Martínez, I. Mártil, D. Bravo, and F. J. López, *J. Appl. Phys.* **87**, 1187 (2000).
- ²⁴E. San Andrés, A. del Prado, I. Mártil, G. González-Díaz, D. Bravo, and F. J. López, *J. Appl. Phys.* **92**, 1906 (2002).
- ²⁵S. García, J. M. Martín, M. Fernández, I. Mártil, and G. González-Díaz, *Philos. Mag. A* **73**, 487 (1996).
- ²⁶F. L. Martínez, I. Mártil, G. González-Díaz, B. Selle, and I. Sieber, *J. Non-Cryst. Solids* **227–230**, 523 (1998).
- ²⁷A. del Prado, F. L. Martínez, M. Fernández, I. Mártil, and G. González-Díaz, *J. Vac. Sci. Technol. A* **17**, 1263 (1999).
- ²⁸A. del Prado *et al.* *J. Appl. Phys.* **93**, 8930 (2003).
- ²⁹W. A. Lanford and M. J. Rand, *J. Appl. Phys.* **49**, 2473 (1978).
- ³⁰G. Lucovsky, *Solid State Commun.* **29**, 571 (1979).
- ³¹J.-L. Yeh and S.-C. Lee, *J. Appl. Phys.* **79**, 656 (1996).
- ³²D. V. Tsu, G. Lucovsky, and M. J. Mantini, *Phys. Rev. B* **33**, 7069 (1986).
- ³³P. G. Pai, S. S. Chao, Y. Takagi, and G. Lucovsky, *J. Vac. Sci. Technol. A* **4**, 689 (1986).
- ³⁴D. V. Tsu, G. Lucovsky, M. J. Mantini, and S. S. Chao, *J. Vac. Sci. Technol. A* **5**, 1998 (1987).
- ³⁵A. Sassella, A. Borghesi, F. Corni, A. Monelli, G. Ottaviani, R. Tonini, B. Pivac, M. Bacchetta, and L. Zanotti, *J. Vac. Sci. Technol. A* **15**, 377 (1997).
- ³⁶S. Hasegawa, S. Sakamori, M. Futatsudera, T. Inokuma, and Y. Kurata, *J. Appl. Phys.* **89**, 2598 (2001).

- ³⁷P. M. Lenahan and J. F. Conley, Jr., *J. Vac. Sci. Technol. B* **16**, 2134 (1998).
- ³⁸J. H. Stathis, J. Chapple-Sokol, E. Tierney, and J. Batey, *Appl. Phys. Lett.* **56**, 2111 (1990).
- ³⁹D. Schalch, A. Scharmann, and R. Wolfrat, *Thin Solid Films* **124**, 301 (1985).
- ⁴⁰K. E. Mattsson, *J. Appl. Phys.* **77**, 6616 (1995).
- ⁴¹A. del Prado, E. San Andrés, F. L. Martínez, I. Mártil, G. González-Díaz, W. Bohne, J. Röhrich, B. Selle, and M. Fernández, *Vacuum* **67**, 507 (2002).
- ⁴²W. L. Warren, J. Kanicki, F. C. Rong, and E. H. Poindexter, *J. Electrochem. Soc.* **139**, 880 (1992).
- ⁴³C. M. M. Denisse, K. Z. Troost, F. H. P. M. Habraken, W. F. van der Weg, and M. Hendriks, *J. Appl. Phys.* **60**, 2543 (1986).
- ⁴⁴E. San Andrés, A. del Prado, F. L. Martínez, I. Mártil, G. González-Díaz, D. Bravo, F. J. López, and M. Fernández, *Vacuum* **67**, 525 (2002).